

Structures and spectroscopy of hexaaquametal(III) ions

James K. Beattie ^{a,*}, Stephen P. Best ^b

^a *School of Chemistry, University of Sydney, Sydney, NSW 2006, Australia*

^b *School of Chemistry, University of Melbourne, Parkville, Vic. 3052, Australia*

Received 21 April 1997; accepted 6 June 1997

Contents

Abstract	391
1. Introduction	392
2. Alums	392
3. Crystal structures	394
3.1. X-ray structures of sulfate alums	394
3.2. X-ray structures of selenate alums	396
3.3. Neutron structures of alums	396
3.4. Hydrogen bonds	398
4. Electronic effects	399
4.1. Anomalous caesium α alums of cobalt, rhodium and iridium	399
4.2. Twist angles relative to the $M^{III}-O_6$ framework	400
4.3. Electron spin distributions	401
4.4. Electronic spectra	404
4.5. Luminescence	405
4.6. Magnetism/EPR	405
4.7. Theoretical calculations	406
5. Vibrational spectra	409
6. Solution structures	411
7. Geometry of the water molecule	412
8. Summary	413
Acknowledgments	413
References	413

Abstract

The hexaaquametal(III) complex ions of transition and Group 13 metals can be isolated in a highly symmetric environment in alum crystals with various monovalent cations and sulphate or selenate anions, $M^I M^{III}(XO_4)_2 \cdot 12H_2O$. Many of these have been investigated by X-ray crystallography and some by neutron scattering. The relationships among the structures are described, with emphasis on the way in which the water molecule is coordinated to the

* Corresponding author.

tervalent metal ion. Both trigonal-planar and trigonal-pyramidal coordination geometries are observed. The structural studies are correlated with electron spin distributions obtained from polarised neutron diffraction, with aspects of the electronic spectra of some of the metal ions, with vibrational spectra, with electron paramagnetic resonance spectroscopy of the titanium alum, and with theoretical calculations. It is concluded that the observed stereochemistry reflects a subtle interplay between the electronic structure of the trivalent metal ion and the hydrogen bonding requirements of the lattice. © 1997 Elsevier Science S.A.

Keywords: Aqua ions; Alums; Coordinated water

1. Introduction

Until 1977 there appears to have been no detailed description of a crystal structure containing the hexaaquairon(III) ion reported in the literature [1], despite the importance of this species in aqueous solution chemistry and the role of the $\text{Fe}^{3+}/\text{Fe}^{2+}$ couple as a model for electron transfer theories [2].

The iron-oxygen bond length difference of 14 pm between $[\text{Fe}(\text{H}_2\text{O})_6]^{3+}$ and $[\text{Fe}(\text{H}_2\text{O})_6]^{2+}$ [3] might be considered relatively large for the difference in the d-electron configurations of $(t_{2g})^3(e_g)^2$ and $(t_{2g})^4(e_g)^2$, one nominally non-bonding t_{2g} electron. Consequently, we sought to determine the difference between the metal-oxygen distances in $[\text{Co}(\text{H}_2\text{O})_6]^{3+}$ and $[\text{Co}(\text{H}_2\text{O})_6]^{2+}$, with d-electron configurations $(t_{2g})^6$ and $(t_{2g})^5(e_g)^2$, i.e. where two anti-bonding e_g electrons are introduced on reduction from Co^{III} to Co^{II} .

Johnson and Sharpe had described a convenient electrochemical preparation of the caesium cobalt sulphate alum in 1966 [4]. They inferred, incorrectly, from the X-ray powder photographs that the caesium cobalt sulphate alum was isomorphous with the vanadium, chromium, manganese, iron and gallium alums, and hence had the cubic β -alum structure. They then measured the unit cell dimension to be 12.277(3) Å, considerably smaller than the value of 12.429(3) Å they found for the iron(III) alum. This would suggest a large effect of the anti-bonding e_g^* electrons. Although they quoted Haussühl [5], they did not recognise that he had predicted on the basis of the crystal morphology, remarkably and correctly as it turns out, that the caesium cobalt sulphate alum belonged instead to the α class of alums. We confirmed this prediction with the determination of the crystal structure of the cobalt alum [6] and were then led to a thorough investigation of the properties of the hexaaquametal(III) ions in the alum lattice.

Whereas a few structural studies have been completed on trivalent hexaaqua cations in other salts, by far the most extensive range of structural data exists for the alums. Hence the structural chemistry of the alums will be discussed in detail and the structures of trivalent hexaaqua cations in other salts will be described in relation to the alums.

2. Alums

The alums comprise compounds of the composition $[\text{M}^{\text{I}}\text{M}^{\text{III}}(\text{XO}_4)_2 \cdot 12\text{H}_2\text{O}]$, where M^{I} and M^{III} may be a wide variety of monovalent and trivalent metal ions,

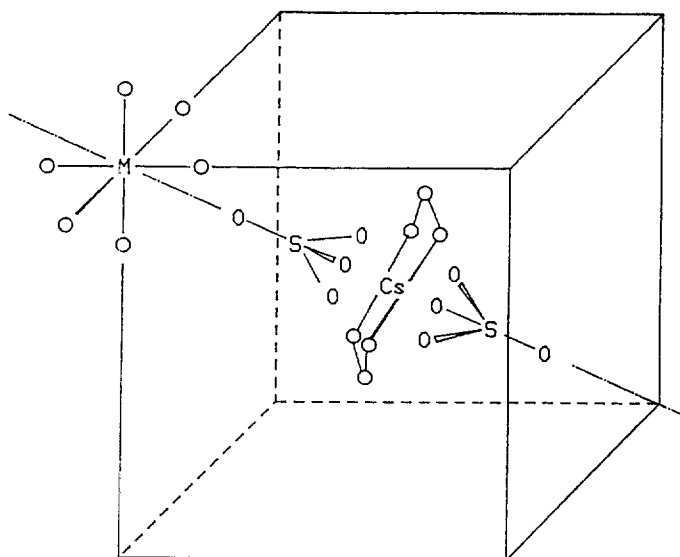


Fig. 1. Subunits of the alum structure.

respectively, and X is a Group 16 element, S or Se. In 1935 Lipson [7] observed that all of the alum structures belong in the same space group $\text{Pa}\bar{3}$, but that they comprise three classes, α , β and γ , determined largely by the size of the univalent ion. Most alums have the α structure; those with large monovalent ions such as caesium adopt the β structure; the only example of the γ structure is with the small sodium ion in $[\text{NaAl}(\text{SO}_4)_2 \cdot 12\text{H}_2\text{O}]$. With the larger selenate anion, only α alums are found.

The differences among these structures can be described by the disposition of the structural subunits along the three-fold crystallographic axis of the cubic unit cell (Fig. 1). The alums comprise monovalent and trivalent hexaaqua cations with intervening divalent anions. The cations occupy sites of S_6 symmetry and the anions occupy sites of C_3 symmetry. The coordination geometry about the trivalent cation is invariably regular octahedral, the axes of which are aligned, approximately, with the unit cell axes. For the α and β alums the coordination sphere of the univalent cation comprises twelve oxygen atoms, six water molecules and six sulphate oxygen atoms from two sulphate groups. According to the alum type the coordination may be described as 12 coordinate (β) in a cuboctahedral array, or 6+6 (α) in an elongated icosahedron. For alums with small univalent cations disorder of the structure occurs, with inversion of a fraction of the sulphate groups along the three-fold axis. This reduces the sulphate from a 3 to a 1 oxygen atom donor. For the γ structure all of the sulphate groups are inverted and the coordination number of the sodium cation is 6+2.

Because the unit cell and site symmetry of the subunits are the same for each of the alum types the classification depends on the details of the structure. The γ alum

is structurally distinct in terms of the orientation of the sulphate groups and can readily be identified. The α and β alum types are more closely related and it was necessary to establish that these modifications represent distinct structural entities rather than a continuum between the limiting structures. The methylammonium sulphate alums of aluminium and chromium display dimorphism [8,9] which suggests that there are distinct energy minima for the two types. Further structural and spectroscopic work described below confirmed that a distinction can be made between the α and β alum types from a variety of observations.

In 1961 Haussühl [5] was able to classify more than fifty alums into the α or β classes on the basis of their crystal morphology. The appearance of a 210 face implied the β structure. His classifications included the unexpected observations that the caesium cobalt sulphate alum, alone among the caesium sulphate alums, belonged to the α instead of the β class, and that all of the titanium and vanadium sulphate alums belong to the β class, even with the smaller potassium and rubidium ions, in contrast with other alums of these monovalent cations which are all in the α class. Our subsequent crystallographic investigations have confirmed all of these remarkable predictions.

3. Crystal structures

3.1. X-ray structures of sulphate alums

Table 1 summarises results from X-ray crystal structure determinations of various sulphate alums. The most reliable guide to the classification of the alum type is the geometry of the six water molecules coordinated to the univalent cation [6]. Since this cation occupies a site of S_6 symmetry there is only one symmetry inequivalent molecule. If the water oxygen atom occupies the plane normal to the three-fold axis which includes the univalent cation then the oxygen atoms of the six symmetry related water molecules will lie in a plane, with $O-M^I-O$ angles of 60.0° . A deviation from the plane will result in angles larger than 60° . For the β alums an $O-M^I-O$ bond angle of $60.0(3)^\circ$ pertains, whereas angles of $65(2)^\circ$ are found for the α alums.

From the tabulated results it is clear that the caesium cobalt sulphate alum belongs unambiguously to the α class, as do the caesium alums of rhodium(III) and iridium(III), in contrast to other caesium alums. It is also clear that the titanium and vanadium alums all belong to the β class, as predicted by Haussühl [5].

The determination of metal–oxygen bond lengths for the hexaaquametal(III) ions was one of the original purposes of this work. These are listed in Table 1 and are plotted in Fig. 2 against the unit cell dimensions. From this plot it can be seen that the α and β alums lie on different lines, so that, contrary to Johnson and Sharpe [4], one cannot make a comparison of bond lengths from the unit cell dimensions of the caesium cobalt and other caesium alums. The distinction between the two classes is further evidence that they are separate structures and not a continuum of structures.

Table 1
X-ray crystal structure determinations of sulphate alums

M^{III}	Unit cell (Å)	Class	O–M ^{III} –O (deg)	M ^{III} –O (Å)	Axes (deg)	Ref.
NaCr	12.40(5)	α	65.8	1.98(1)	8.2	[75]
KAl	12.157(3)	α	66.5	1.908(8)	10.2(3)	[76]
KV ^a	12.253(5)	β	60.03(3)	1.992(1)	0.69(4)	[36]
RbAl	12.243(3)	α	65.9(2)	1.923(9)	8.3(4)	[76]
RbV	12.367(2)	β	60.0(1)	1.996(3)	0.7(1)	[36]
RbCr	12.30(6)	α	64.6	1.88(1)	8.0	[9]
CsAl	12.357(6)	β	60.03(11)	1.877(3)	0.8(1)	[6]
CsTi	12.393(5) ^b	β	60.0	2.028(5)	0.2	[57]
CsV	12.452(10)	β	60.0(2)	1.992(6)	0.8(1)	[6]
CsV	12.434(1)	β	60.00(2)	1.991(1)	0.70(4)	[36]
CsCr	12.413(5)	β	60.01(10)	1.959(3)	0.8(1)	[6]
CsMn	12.432(8)	β	60.0(1)	1.991(6)	0.8(1)	[6]
CsFe	12.449(3)	β	60.0(1)	1.995(4)	0.9(1)	[6]
CsCo	12.292(8)	α	65.5(2)	1.873(5)	2.2	[6]
CsGa	12.419(3)	β	60.01(9)	1.944(3)	0.5(1)	[6]
CsRh	12.357(5)	α	65.3	2.016(3)	2.2	[77]
CsIn	12.540(7)	β	60.0(1)	2.112(4)	1.0(1)	[6]
CsIr	12.395(3)	α	65.3	2.041(3)	2.9	[77]
NH ₄ Al	12.240(3)	α	66.2(2)	1.916(8)	9.1	[76]

^a 120 K.

^b 101.5 K.

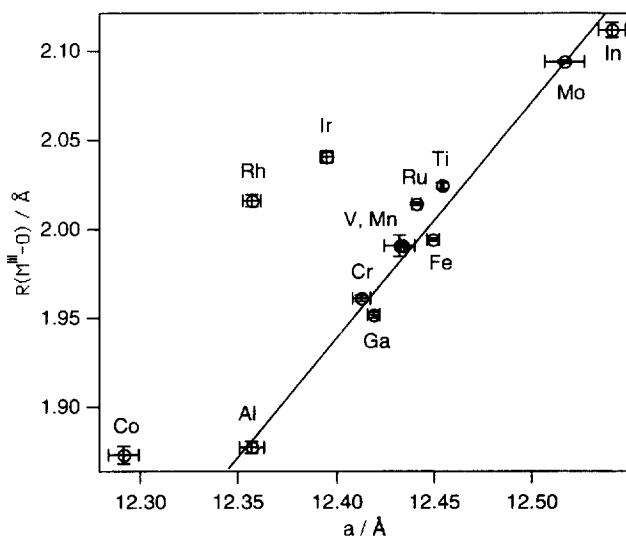


Fig. 2. Metal(III)–oxygen distances as a function of the unit cell dimension of the sulphate alums.

3.2. X-ray structures of selenate alums

Table 2 gives some results from the X-ray crystal structure determinations of some caesium selenate alums. With the larger selenate anion all of the caesium alums adopt the α alum structure. Two important points emerge from these results.

(1) There are no significant differences between the $M^{III}-O$ bond distances observed for the caesium sulphate β alum and the caesium selenate α alum of the same transition metal (Table 2). This shows that the difference between the α and β structures does not perturb the M^{III} –water bond significantly. This is consistent with the similarities between the vibrational spectra of the two alum types [10] and with the small energy difference between the two structures, both to be described below.

(2) The $M^{III}-O$ bond length and bond strength (implied by the $M-O$ distance and its vibrational frequency) are also not affected by the subtleties of the orientation of the coordinated water. In most caesium β sulphate alums the MO_6 moiety is oriented with the $M-O$ coordination axes within one degree of the crystallographic axes. In contrast, in the α alums the $M^{III}-O$ axes are $4-7^\circ$ away from the crystallographic axes, which accommodates the different hydrogen-bonded layout of the α alums. In contrast, both the sulphate α and the selenate α alum of rhodium belong to the same polymorph, and have the same unique orientation of 2.2° to the crystal axes. In each case, however, the bond length and its vibrational frequency are not different between the sulphate and selenate alums. This indicates that the $M^{III}-O$ bond length and bond strength are not significantly affected by the precise orientation of the coordinated water.

3.3. Neutron structures

An early neutron diffraction structure determination was made of the potassium chromium sulphate alum in 1958 [11]. One of us has reported a number of recent studies, which are summarised in Table 3. By locating the hydrogen atoms, neutron diffraction is able to examine the geometry of the water coordination; an important question is whether the water is essentially planar (sp^2 hybridised at the oxygen) or pyramidal (some sp^3 hybridization character).

Table 2
X-ray crystal structure determinations of selenate alums [78]

$M^{III}M^{III}$	Unit cell (Å)	Class	$O-M^{III}-O$ (deg)	$M^{III}-O$ (SeO_4) (Å)	$M^{III}-O$ (SO_4) (Å)	Angle of $M^{III}O_6$ to crystal axes (deg)	
						SO_4	SeO_4
CsAl	12.544(3)	α	66.6	1.878(3)	1.877(3)	0.8	6.5
CsCr	12.575(3)	α	66.2	1.964(3)	1.959(3)	0.8	4.6
CsFe	12.615(5)	α	66.2	1.989(4)	1.995(4)	0.9	5.4
CsRh	12.532(7)	α	65.7	2.004(3)	2.016(3)	2.2	2.2
CsIn	12.694(6)	α	65.6	2.134(6)	2.112(4)	1.0	3.9

Table 3
Neutron diffraction structure determinations of alums

Compound	Alum class	Tilt angle (deg)	Twist angle (deg)	Ref.
KCr(SO ₄) ₂ · 12H ₂ O	α			[11]
CsAl(SO ₄) ₂ · 12H ₂ O	β			[79]
NaAl(SO ₄) ₂ · 12H ₂ O	γ			[80]
NH ₄ Al(SO ₄) ₂ · 12H ₂ O	α	15.5(8)	0.8(8)	[81]
CsFe(SO ₄) ₂ · 12H ₂ O	β	0	−19.4(6)	[13]
CsFe(SeO ₄) ₂ · 12H ₂ O	α	18.6	0	[13]
CsRu(SO ₄) ₂ · 12H ₂ O	β	0.8(6)	−22.0(6)	[17]
CsCr(SO ₄) ₂ · 12H ₂ O	β	0.8(6)	−19.0(4)	[14]
CsV(SO ₄) ₂ · 12H ₂ O	β	1	−20	[78]
CsRh(SO ₄) ₂ · 12H ₂ O	α	35	0	[78]
CsMo(SO ₄) ₂ · 12D ₂ O	β	0	−19.7(1)	[82]
CsRu(SO ₄) ₂ · 12D ₂ O	β	0	−22.0(2)	[82]
CsTi(SO ₄) ₂ · 12H ₂ O ^a	β	0.6(3)	−20.5(3)	[57]

^a Neutron powder data.

In a definitive study published in 1984, Cotton and co-workers reported a neutron diffraction determination of the structure of [V(H₂O)₆][H₅O₂](CF₃SO₃)₄ [12]. They observed that there are three highly symmetric structures possible with planar water, illustrated in Fig. 3: (a) T_h symmetry; (b) all-vertical D_{3d} symmetry; and (c) all-horizontal D_{3d} symmetry. The last is also possible with pyramidal coordinated water. In [V(H₂O)₆][H₅O₂](CF₃SO₃)₄ the water molecules are nearly planar and adopt the all-horizontal D_{3d} configuration.

In the alums the hexaaquametal(III) ion occupies a site of S₆ symmetry. Both planar and pyramidal coordination of the water are observed. The degree of deviation from planar coordination can be defined by the “tilt” angle – the angle made between the plane of the water molecule and the M–O bond. For planar water this is 0°; in a tetrahedron this angle is 54.35°. The tilt angles found in a number of the neutron structures are given in Table 3.

A key difference between the α and β alum types is the orientation of the coordinated water molecule relative to the M^{III}O₆ framework. A twist angle (φ) is defined as the angle between the plane of the water molecule and the closer MO₄ plane which includes its oxygen atom; this is illustrated in Figs. 3e and 3f. The sign of the twist angle is defined with respect to the C₃ axis of the octahedron. Thus rotation of the plane of the water from the T_h geometry (φ = 0) towards the C₃ axis and the all-vertical D_{3d} geometry is positive, and rotation towards the all-horizontal D_{3d} geometry is negative (see Fig. 5). In the α alums the plane of the water molecule is approximately aligned with the MO₆ framework; in the β alums a twist angle, φ, of between −17 and −22° is found. The stereochemistry of the cation in the α alums is approximately midway between T_h (plane of the water molecules aligned with the O_h axes, φ = 0°) and the *all-horizontal* D_{3d} geometry (plane of the water molecules normal to the σ_v planes in D_{3d}, φ = −45°).

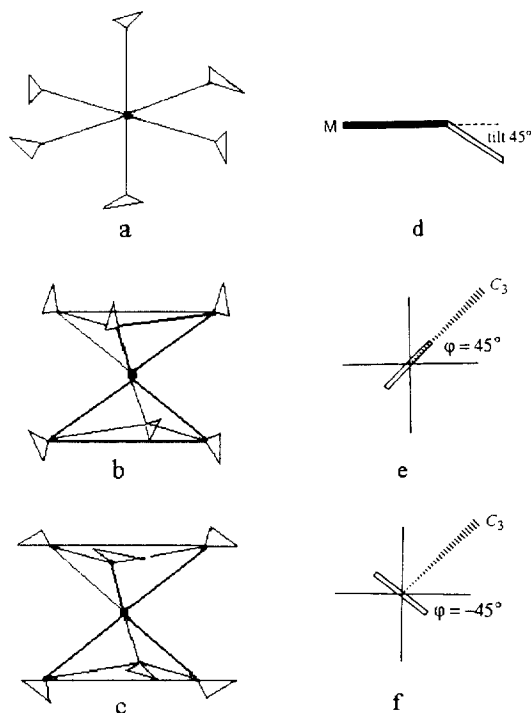


Fig. 3. Highly symmetric arrangements of planar coordinated water. After Cotton, *et al.* [12]: (a) T_h symmetry; (b) all-vertical D_{3d} ; (c) all-horizontal D_{3d} ; (d) definition of the tilt angle; (e) definition of positive twist angle ϕ for all-vertical D_{3d} ; and (f) negative twist angle for all-horizontal D_{3d} .

The third angle required to analyse the geometry of the coordinated water is the orientation of the MO_6 octahedron relative to the crystal axes. These are given in Table 1. In the β alums the MO_6 octahedron is aligned to within about one degree with the crystal axes. In the α alums it is rotated by 5–10° away from the crystal axes, except in the anomalous caesium α alums of cobalt, rhodium and iridium.

3.4. Hydrogen bonds

There are four hydrogen bonds in the asymmetric unit of the alum lattice, illustrated in Fig. 4. For the caesium iron selenate (α) and the caesium iron sulphate (β) alums for which high quality neutron structures have been determined, the hydrogen bonds of the water molecules coordinated to the tervalent cation are the strongest in the lattice: they have the longest O–H bond lengths and the shortest O...O distances [13]. These hydrogen bonds are close to linear. They are directed to the water oxygen (O(a)) and the anion oxygen (O(2)) which comprise the coordination sphere of the univalent cation. They link the geometry about the univalent cation, and thus the alum type, with the orientation of the water of the tervalent cation.

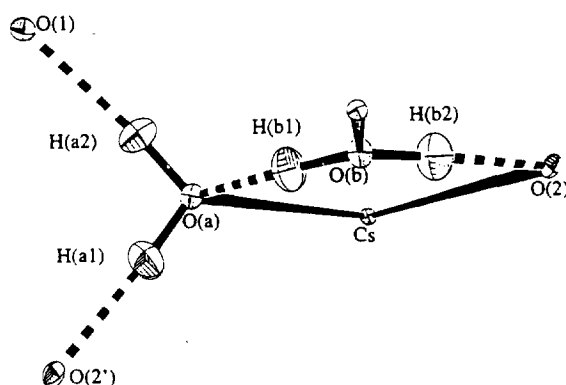


Fig. 4. Hydrogen bonds in alums. O(b) coordinated to the trivalent cation is hydrogen-bonded to O(2) of the anion and O(a) of the water coordinated to the monovalent cation.

4. Electronic effects

The initial explanation of the different alum classes was based on the size of the univalent cation: the very small sodium ion adopts the γ structure so that its coordination number is only eight; the intermediate potassium and rubidium alums adopt the α structure with a puckered crown of six waters; the largest caesium ion adopts the β structure with a plane of six waters, which creates a larger coordination sphere than the puckered crown. Haussühl's classification based on crystal morphology was not consistent with this simple model [5]. Our structure determinations confirm the predicted exceptions and indicate that the structure can be affected by the electronic structure of the trivalent cation, in addition to the size of the univalent cation. The relationships among the coordination geometry of the trivalent water (the tilt and twist angles), the orientation of the trivalent octahedron in the lattice, and the coordination geometry of the univalent cation (alum class) requires a fascinating analysis of electronic and steric effects.

4.1. Anomalous caesium α alums of cobalt, rhodium and iridium

Most caesium alums adopt the β structure, but those of the $(t_{2g})^6$ metal ions cobalt(III), rhodium(III) and iridium(III) have the α structure. This cannot be related to the sizes of the trivalent ions, which span most of the observed range from Al to In (Fig. 2). These caesium alums are also unique among the α alum structures. The typical α alum has the MO_6 octahedron oriented about 5 – 10° away from the crystal axes; in the caesium α alums this angle is only 2 – 3° . The hydrogen bond directions required to accommodate the α alum structure are accomplished by a very large tilt angle of 35° , i.e. the trivalent coordinated water is highly pyramidal, or sp^3 hybridised, compared with the usual coordination which is close to planar (β alums) or 15 – 20° (other α alums).

One hypothesis advanced to explain this anomaly is that the pyramidal coordina-

tion occurs to minimise electron repulsions between the oxygen lone pair and the filled metal t_{2g} orbitals. Such repulsion must be of modest energy, for it has no effect on the $M^{III}-O$ bond lengths among the first row transition metals; the Co–O distance occurs as predicted by extrapolation from earlier members of the 3d series, with fewer t_{2g} electrons (Fig. 2 in Ref. [6]). This is consistent, however, with the small energy difference between the α and β structures estimated from electronic effects to be described below, and the independence of the $M^{III}-O$ distance on alum type described above in the comparison between the sulphate and selenate alums.

Among the 4d metals, only Mo, Ru and Rh structures are available. In this case the Rh–O distance is longer than predicted from the two-point extrapolation of the Mo and Ru distances (Fig. 2). If this comparison were valid, it might reflect the greater radial extent of the 4d than the 3d electrons.

If this hypothesis were correct, it might be expected the $Ru^{III}(t_{2g})^5$ would also adopt the α structure, but there are additional factors involved with this electron configuration which complicate such a prediction. This involves the role of $p_{\pi}-d_{\pi}$ bonding in the planar coordination of water, which is absent in Rh and which can also affect the orientation and twist angle of the coordinated water.

4.2. Twist angles relative to the $M^{III}-O_6$ framework

Whereas the hydrogen bonding framework plays an extremely important role in determining the orientation of the water molecules, the metal(III)–water interactions also perturb the structures at a level which is revealed in the precise neutron structure determinations. The three-fold degeneracy of the t_{2g} orbitals in octahedral symmetry is lifted in the S_6 site of the alum lattice. The relationship between the angle that the plane of the water molecule makes to the O_h axes and the energy difference between the a_g and e_g (S_6) components of the t_{2g} (O_h) orbitals is shown in Fig. 5 [14]. Orbital energies were calculated using Eq. (1) which is derived from the angular overlap model (AOM) [15,16] assuming (i) trigonal-planar coordination of the water molecule, (ii) S_6 symmetry, (iii) metal–ligand π interaction greater normal to the plane than in the plane of the water molecule, and (iv) neglect of configuration interaction

$$\delta = |3e_{\pi} \sin(2\phi)| \quad (1)$$

where δ is the absolute magnitude of the trigonal-field splitting and e_{π} is an AOM parameter related to the difference in the metal–ligand π interaction normal to and in the plane of the water molecule.

The tervalent cations can be grouped according to the electronic stabilisation gained by the lifting of the degeneracy of the metal t_{2g} orbitals by a change of ϕ : (1) where there is equal occupancy of the metal t_{2g} orbitals, there is no preferred twist angle; (2) $(t_{2g})^2$ and $(t_{2g})^5$ cases for which the electronic minimum occurs with $\phi = -45^\circ$; and (3) $(t_{2g})^1$ and $(t_{2g})^4$ cases where the electronic minimum occurs with $\phi = +45^\circ$. In the case of chromium(III) there is no electronic stabilisation energy to be gained by adopting a particular value of ϕ since each of the t_{2g} derived orbitals

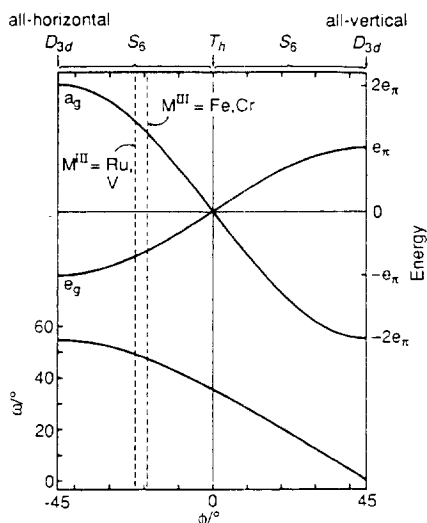


Fig. 5. Relationship between molecular structure and orbital energies. Top: relative energies of the a_g and e_g components of the t_{2g} orbitals; and bottom: relationship of twist angle ϕ and angle ω made between the plane of the water molecule and three-fold axis of the octahedron.

are singly occupied. The observed twist angle of $-19.0(4)^\circ$ [14] is, within experimental error, also that found for the corresponding iron alum ($19.4(3)^\circ$) [13] where similar considerations apply to the $(t_{2g})^3(e_g)^2$ configuration. For the ruthenium(III) cation, the $(t_{2g})^5$ configuration achieves its maximum electronic stabilisation energy when $\phi = -45^\circ$. In this case the observed twist angle of $-22.5(3)^\circ$ [17] is a compromise between the electronic factor and the hydrogen bonding requirements of the alum lattice.

A recent high resolution powder neutron diffraction study of $\text{CsTi}(\text{SO}_4)_2 \cdot 12\text{D}_2\text{O}$ has permitted the characterisation of the coordination geometry of $[\text{Ti}(\text{OD}_2)_6]^{3+}$. In this case the twist angle is $-20.5(3)^\circ$, between that obtained for the case where $\text{M}^{\text{III}} = \text{Cr}$ and Ru . For the d^1 case the global minimum of the electronic energy corresponds to a twist angle of $+45^\circ$; however, within the hydrogen bonding network of the alums it is energetically more favourable to distort towards a local (-45°) rather than a global minimum in the electronic energy. On this basis the more negative twist angle observed for the $\text{CsTi}(\text{SO}_4)_2 \cdot 12\text{D}_2\text{O}$ alum than for the corresponding Cr salt is consistent with the simple analysis outlined above. It is clear that hydrogen bonding considerations are important and the relative magnitudes of the twist angle observed for the Ti and Ru alums reflects the subtle balance of electronic, hydrogen bonding and steric factors.

4.3. Electron spin distributions

A key assumption of this analysis is the presence of a significant and anisotropic metal–water π interaction. The π bonding characteristics of water as a ligand have

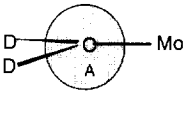
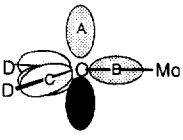
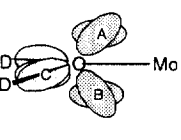
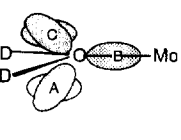
been the source of some uncertainty and it is important to establish a physical basis for such an interaction. In principle this may be obtained from the charge density about the metal–ligand bond or, for paramagnetic complexes, from the spin density within the complex. While there have been significant advances in the extraction of charge densities from low-temperature X-ray scattering experiments, the small perturbations to the charge distribution which result from bonding interactions must be extracted from the total scattering which contains contributions from all the electrons in the unit cell. The spin distribution gives the spatial distribution of the unpaired electrons and, in cases where the bonding orbitals are involved, the measurement provides a sensitive probe of the bonding interactions. Experimentally, the spin distribution may be obtained indirectly from analysis of the hyperfine couplings of the ESR spectra [18] or, more directly, from magnetic structure factors obtained by single crystal polarized neutron diffraction (PND) [19,20]. PND measurements have been reported for $[\text{Mo}(\text{OD}_2)_6]^{3-}$ in the caesium sulphate salt [21]. In an octahedral environment the three unpaired electrons of molybdenum(III) occupy the t_{2g} orbitals: therefore the spin distribution ought be sensitive to the extent and spatial distribution of the metal–water π bonding.

The spatial distribution of the magnetic moment within the unit cell may be obtained from the Fourier transform of the magnetic structure factors. Where there is no contribution to the magnetic moment from the orbital angular momentum this corresponds to the spin distribution [22]. Owing to limitations in the extent of data collection, analysis of the PND data is best completed within the framework of orbital-based models [23,24], although more recent work involving the use of maximum entropy techniques may permit extraction of model-independent spin distributions [25]. In view of the importance of the characterisation of the metal–ligand π interactions for the trivalent hexaaqua cations the least squares fits of the PND results from $\text{CsMo}(\text{SO}_4)_2 \cdot 12\text{D}_2\text{O}$ will be described [21].

Fits of the most important orbital-based models of the spin distribution about the oxygen atom to the PND data are given in Table 4. In each case the spin on the metal is modelled by 4d orbitals of appropriate symmetry (a_g , e_π and e_σ) and a diffuse Mo-centred 5s orbital. The high quality of the fit of the experimental results obtained using only the metal-centred functions and an isotropic function centred on the oxygen atom (model 1) reflects the concentration of the spin (ca. 90%) in metal 4d- t_{2g} (O_h) orbitals. The extent to which the experiment can give insight into the details of the metal–water bonding interaction must be assessed in terms of the improved quality of fit obtained with the orbital models used to describe the spin distribution about the oxygen atom. In terms of the coordination geometry of the oxygen atom the most appropriate orbital description of the oxygen site may be either sp^2 (model 2), based on the trigonal-planar coordination geometry about the oxygen atom, or sp^3 (models 3 and 4), based on the H–O–H bond angle (111.1°). In terms of chemical intuition the sp^2 -based model would seem most reasonable and the R factor and goodness of fit obtained in this case is the best obtained of all the models examined and is a sufficient improvement on a simple isotropic function (model 1) to justify the modelling of the spin anisotropy about the oxygen atom. The contributions to the magnetisation given by model 2 (sp^2) show that the

Table 4

Magnetisation populations obtained from fitting the PND results of $\text{CsMo}(\text{SO}_4)_2 \cdot 12\text{D}_2\text{O}$

				
Model	1 (2s)	2 (sp^2)	3 (sp^3)	4 (sp^3)
$e_g(\sigma)$	-0.05(3)	-0.03(2)	-0.04(3)	-0.03(2)
$e_g(\pi)$	1.76(3)	1.69(3)	1.75(3)	1.70(3)
a_g	1.07(2)	1.02(2)	1.05(2)	1.02(2)
4d radial	1.078(4)	1.068(4)	1.076(4)	1.069(4)
5s	-0.20(4)	-0.10(4)	-0.16(4)	-0.08(4)
5s radial	1.1(1)	1.6(3)	1.1(1)	1.6(4)
Orbital A	0.027(2)	0.035(5)	0.015(3)	0.020(3)
Orbital B	-	-0.017(3)	-0.002(4)	-0.013(3)
Orbital C	-	0.003(2)	0.007(2)	0.010(2)
$D_1(1s) =$ $D_2(1s)$	0.009(2)	0.009(2)	0.007(2)	0.006(2)
R_w	0.0382	0.0317	0.0370	0.0333
χ^2	1.48	1.23	1.44	1.29

2p-orbital, which is normal to the plane of the water molecule, has a well-defined and significant occupation whereas the two hybrid orbitals which lie in the water plane and which point toward the deuterium atoms have well-defined but insignificant populations. The significant negative occupation of the hybrid orbital directed at the molybdenum atom is attributed to spin polarisation, an effect which has been commonly observed in the PND studies of divalent hexaaqua cations [26–30].

When sp^3 hybrid orbitals are used to model the spin density about the oxygen atom, there are choices for the directions of the quantisation axes as shown for models 3 and 4 in Table 4. Model 3 has two hybrid orbitals directed along the O–D bonds and this leaves the remaining hybrid orbitals disposed above and below the Mo–O bond. In this model no orbitals are available to describe the significant spin

density along the Mo–O bond and the χ^2 and R_w values are significantly higher than those of model **2** where a sp^2 hybrid orbital is available to describe the spin polarisation which results from the Mo–O bonding interaction, and are little better than those of model **1** where a single s orbital is used to model the spin on the atom. Alternatively, one sp^3 hybrid orbital may be directed along the Mo–O bond and the other three such orbitals disposed so as to preserve a local plane of symmetry normal to the plane of the water molecule. While the small tilt of the plane of the coordinated water molecule relative to the Mo–O bond vector (1.8°) leads to two inequivalent arrangements this effect has only a marginal effect on the quality of the fits obtained, the better fit is given in Table 4. Neither of the sp^3 fits of the data (models 3 and 4) have a satisfactory relationship with the molecular framework. The significant spin in the Mo–O interbonding region and insignificant spin in the O–D bonds results in a considerably better fit for model 4.

For both the sp^2 and sp^3 models there is clear evidence of anisotropy of the spin distribution of the Mo–O bond. However, in both cases the choice and disposition of the orbitals on the oxygen atom permit description of the Mo–O π bonding normal to the plane of the water molecule but not in it. It is important to establish that the conclusions of the analysis are not determined by the form of the models. Accordingly, the models were extended by the inclusion of orbitals which would describe the spin transfer to the oxygen atom as a result of in-plane Mo–O π bonding. Model **2** was extended by the addition of an oxygen 2p-orbital normal to the Mo–O bond and parallel to the plane of the water molecule located at (a) the oxygen atom, (b) 75% of the Mo–O bond length and (c) the midpoint of the bond. In all three cases the population of the additional orbital remained below the 1 e.s.d. level and the quality of the fit of the experimental data was not improved significantly. This observation was taken to imply that there is no significant Mo–O π interaction in the plane of the water molecule.

In summary the PND results for $[Mo(OD_2)_6]^{3-}$ in $CsMo(SO_4) \cdot 12D_2O$ provide direct evidence for a significant and anisotropic Mo–O π interaction [21]. This observation supports the analysis of the structural chemistry of the alums in terms of the metal–ligand π interactions. As shown in the following sections this conclusion is consistent with analysis of the electronic spectra and magnetism of the alums as well.

4.4. Electronic spectra

The alums have been used as a convenient vehicle for the examination of the electronic spectra of hydrated metal trivalent cations [31–33]. The analysis of the low-temperature electronic spectra of $NH_4V(SO_4)_2 \cdot 12H_2O$ by Hitchman and co-workers [34] revealed that the vanadium(III) cation is subject to a surprisingly large trigonal field considering that the VO_6 framework is little distorted from octahedral. A satisfactory fit of the spectra could be obtained using a trigonal-field splitting of 1950 cm^{-1} . This is comparable with the value of 1940 cm^{-1} suggested by the electronic Raman band attributed to the intra- t_{2g} transition (${}^3E_g \leftarrow {}^3A_g$) of vanadium(III) in a range of β alums [35]. Angular overlap model calculations showed that the trigonal field could not be attributed to a distortion of the VO_6

framework but required the inclusion of metal–ligand π interactions which are different in- and normal to- the plane of the ligand [34].

An estimate of the energy difference between the α and β alum structures can now be made from this estimate of the trigonal-field splitting. The argument is that the potassium and rubidium–vanadium alums would adopt the customary α structure were it not for the additional electronic stabilisation provided in the d^2 electronic configuration by the trigonal-planar coordination of the β structure. This stabilisation is $2/3$ of the trigonal splitting or about 1300 cm^{-1} or 15 kJ mol^{-1} . This can be taken as an upper limit of the energy difference between the α and β structures for the potassium and rubidium–vanadium sulphate alums [36].

4.5. Luminescence

The ${}^2E_g \rightarrow {}^4A_{2g}$ luminescence of chromium(III) in a series of pure and doped alums provides additional insight into the metal–ligand π interaction. The 2E_g excited state is split by spin–orbit coupling between the 2E and 2T_2 states in the presence of a trigonal field and the magnitude of the splitting is related to the strength of the trigonal field [37]. When chromium is doped into α alums the magnitude of the splitting is small ($<10\text{ cm}^{-1}$) [38,39] whereas splittings of the order of $125\text{--}130\text{ cm}^{-1}$ are obtained for chromium(III)-doped β alums [38]. The magnitude of the splitting is dominated by the alum type and not by the size of the tervalent cation of the host lattice. The mean origin energy of the ${}^2E_g \rightarrow {}^4A_{2g}$ transition is also found to depend on the alum type, with energies of ca. $14\,950$ and $14\,540\text{ cm}^{-1}$ respectively, for α and β alums [38]. The lower transition energy for the β alums suggests lower interelectron repulsion such as would result from greater delocalisation. This is consistent with a reduction in $d\pi\text{--}p\pi$ overlap as the plane of the coordinated water molecule is tilted away from the $M\text{--}O$ bond vector. These results show very clearly that the magnitude of the trigonal field at the M^{III} site of the alums is highly sensitive to the orientation of the plane of the coordinated water molecule and not to small distortions of the $M^{III}O_6$ framework. Moreover, it is clear that the relative σ and π character of the metal–water interaction depends strongly on the orientation of the coordinated water molecule.

4.6. Magnetism/EPR

Many of the early experimental studies of the magnetic properties of transition-metal complexes have been conducted on tervalent hexaaqua cations in the alums. These have been described in many of the classic texts on the subject [40–43]. One aspect of this work which merits further consideration concerns the cases where there is unequal occupancy of the t_{2g} (O_h) orbitals. In these cases the temperature dependence of the magnetic moment may be used to extract the trigonal-field splitting. Although these estimates suffer from overparameterisation, the trigonal-field splitting of $[V(OH_2)_6]^{3+}$ deduced from magnetic measurements of the ammonium sulphate alum [44] is in close agreement with that obtained from electronic Raman measurements [35].

A problem which has persisted in the literature since the 1930s has involved the interpretation of the magnetism and EPR spectra of $\text{CsTi}(\text{SO}_4)_2 \cdot 12\text{H}_2\text{O}$. Numerous models of the electronic structure of $[\text{Ti}(\text{OH}_2)_6]^{3+}$ have until recently assumed that the trigonal symmetry of the tervalent cation is retained over the whole of the experimental temperature range and that the trigonal field lowers the orbital degeneracy of the ${}^2\text{T}_{2g}(\text{O}_h)$ ground term to give an orbitally nondegenerate (${}^2\text{A}_g$) ground term [44–56]. This analysis implies that the effect of the trigonal field on the relative energies of the orbitals which comprise the $\text{t}_{2g}(\text{O}_h)$ set is different for the titanium and vanadium alums. Since the caesium sulphate alums of titanium and vanadium are isostructural [6,57] this would imply that the principal metal–water π interaction is normal to the plane of the water molecule for vanadium and in the plane for titanium. Such a proposition is inconsistent with the above interpretation of metal–water π bonding [21]. The assumption that the trigonal field acts on the titanium(III) to give an orbitally nondegenerate ground term is based on the magnetic properties of the Kramers doublet which arises from the ${}^2\text{T}_{2g}$ term after perturbation by spin–orbit coupling and the action of an axial ligand field. If the $[\text{Ti}(\text{OH}_2)_6]^{3+}$ is axially symmetric then a ${}^2\text{E}_g$ ground term would give a g_{\perp} value of zero. The observed value of g_{\perp} (1.14) [46] has been taken to exclude the possibility of a ${}^2\text{E}_g$ ground term. This anomaly has recently been resolved. The assumption that the tervalent cation retains trigonal symmetry over the experimental temperature range (1.5 to 300 K) has been shown to be in error [58]. High resolution powder neutron diffraction experiments have permitted the characterisation of a phase transition of $\text{CsTi}(\text{SO}_4)_2 \cdot 12\text{D}_2\text{O}$ to an orthorhombic phase with a transition temperature of 12 K. Low temperature single crystal Raman measurements of the pure salt and of the analogous rubidium alum and EPR studies of chromium(III)-doped $\text{CsTi}(\text{SO}_4)_2 \cdot 12\text{H}_2\text{O}$ are consistent with the structural measurements. In the low temperature orthorhombic phase the site symmetry of the titanium(III) cation is reduced to C_1 , that is the three-fold symmetry of the alum site is lost. The apparent axial symmetry of the g tensor and the observed magnitudes may be explained using a simple model in which the trigonal field leaves a ${}^2\text{E}_g$ ground term which is then subject to Jahn–Teller distortion. Long-range interaction between the Jahn–Teller centres ultimately results in a cooperative Jahn–Teller effect and the observed phase transition of the crystal [58]. The anomalous fine structure observed in the EPR spectra of Ti^{III} as an impurity in β alums has also been calculated on the basis of the trigonal field giving rise to a ${}^2\text{E}_g$ ground term with coupling strength and low-symmetry strain as parameters in the analysis [59]. The important conclusion from this analysis is that a self-consistent interpretation of the electronic structure of the tervalent cations is possible based on the coordination geometry of the metal, the orientation of the coordinated water molecule relative to the MO_6 framework, and the inclusion of significant and anisotropic metal–water π interaction in cases where the mode of water coordination is trigonal-planar.

4.7. Theoretical calculations

A number of approximate (ligand field/AOM [15], Fenske–Hall [12], extended Hückel [15]) and higher level (multiple scattering X_α [15], ab initio MO [60–63])

calculations have been reported for trivalent hexaaqua cations with a view to resolving the electronic structure or elucidating trends in the physical properties or the mechanism of exchange reactions [62,64,65]. The observed trigonal-planar mode of water coordination and near all-horizontal D_{2d} geometry of $[V(OH_2)_6]^{3+}$ in $[VOH_2)_6][H_5O_2][CF_3SO_3]$ led Cotton to consider the effect of metal–water π interactions on the electronic effects associated with partial occupancy of the metal t_{2g} (O_h) orbitals [12]. Through simple consideration of ligand-field effects, supported by Fenske–Hall calculations, it was concluded that for an octahedral MO_6 arrangement the ligand-field stabilisation energy would be at a maximum for d^1 cations when the geometry is *all vertical* D_{3d} , for d^2 cations when the geometry is *all-horizontal* D_{3d} and there should be no preferred twist angle for d^3 cations. These conclusions were supported by Daul [15] based on MS- X_α and extended Hückel calculations of $[Ru(OH_2)_6]^{3+}$.

The trigonal-field splitting calculated for the complex with *all-horizontal* D_{3d} geometry by the X_α methods was 4900 cm^{-1} and this permitted an estimate of the AOM parameter e_π of 1633 cm^{-1} [15]. The magnitude of the trigonal-field splitting for Ru^{III} in the caesium sulphate alum, 2500 cm^{-1} , was deduced from earlier EPR measurements [66]. The authors [15] assumed, incorrectly, that the M^{III} site symmetry of the alums to be C_3 and not S_6 ; this complicates the AOM-derived expression relating the twist angle to the trigonal-field splitting. If the expression given in Section 4.2 is used to calculate the twist angle then a value of -16° is obtained, in tolerable agreement with that obtained for $CsRu(SO_4)_2 \cdot 12H_2O$ by neutron diffraction (-22°) [17]. It is probably more appropriate to use the trigonal-field splitting and the twist angle to estimate the trigonal-field splitting for the *all-horizontal* D_{3d} geometry of $[Ru(OH_2)_6]^{3+}$. The value of 3675 cm^{-1} thereby obtained may be compared with the value of 4900 cm^{-1} given by the X_α calculations.

A clear focus of a number of the calculations has been the interpretation of the electronic structure of $[Ti(OH_2)_6]^{3+}$ in the caesium sulphate alum [63] with the view of resolving the anomalous g values observed in these experiments. Ab initio SCF MO calculations have been completed on $[Ti(OH_2)_6]^{3+}$ to give optimised structure predictions and this has been supplemented by the calculation of the electronic structure for several fixed structures [60]. In keeping with the simple analysis of the system the *all-vertical* D_{3d} geometry is predicted to be the most stable in terms of electronic effects. The EPR and ENDOR spectra of titanium(III) doped into methanol/water glasses are consistent with this interpretation [67]. The interpretation of the EPR spectra of titanium(III) in the caesium sulphate alum was not resolved by the theoretical work where, although the dependence of the trigonal-field splitting on the twist angle is evident in these calculations, failure to allow for the possibility of low temperature distortions [67] invalidates the analysis.

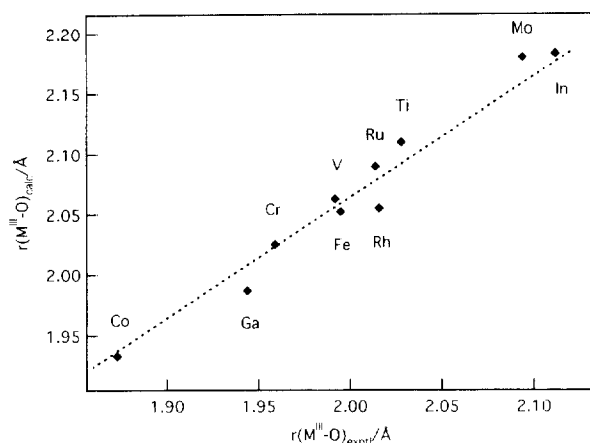
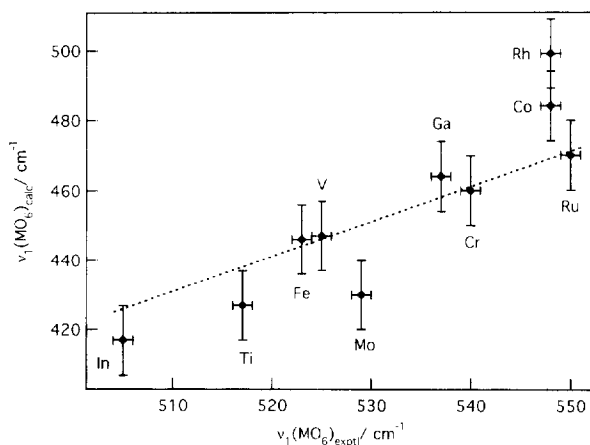
While the cooperative Jahn Teller effect operating in $CsTi(SO_4)_2 \cdot 12H_2O$ may have some effect on the structural parameters obtained for the cubic phase, the larger twist angle observed for Ti than Cr or Mo in the caesium sulphate alums is consistent with an increase in the electronic stabilisation with an increased magnitude of the twist angle. Within the alums the hydrogen bonding arrangement appears to require twist angles of approximately 0° (α) or -20° (β). The negative value of the

twist angle corresponds to the distortion of the d^1 complex towards a local electronic energy minimum, with the Jahn–Teller effect giving a more negative twist angle for titanium, consistent with the structural data.

Calculations have been performed for a number of transition-metal hexaaqua cations to compare the T_h , *all-horizontal* and *all-vertical* D_{3d} symmetries [60]. Whereas electronic factors favour the adoption of *all-vertical* D_{3d} geometry when the metal has a d^1 -electron configuration hydrogen-hydrogen repulsions operate in favour of the T_h geometry. For Ti^{III} the *all-vertical* D_{3d} geometry was calculated to be 3.5 kJ mol^{-1} less stable than the T_h geometry. For larger d^1 cations the opposite result was obtained. It was noted by the authors that MR-SDCI level calculations on an isolated $[Ti(OH_2)_6]^{3+}$ complex gave the *all-vertical* D_{3d} geometry as the lowest energy. Similar conclusions were obtained for the adoption of *all-horizontal* geometry by d^2 cations, i.e. V^{III} was calculated to be 5.8 kJ mol^{-1} more stable in the T_h geometry but larger d^2 cations were calculated to be more stable in the *all-horizontal* D_{3d} geometry. These results were interpreted to indicate that external factors such as hydrogen bonding are responsible for the adoption of near *all-horizontal* D_{3d} geometry of $[V(OH_2)_6]^{3+}$ in the triflate salt [12]. The structural chemistry of the titanium [57,58] and vanadium [36] alums described above argues strongly against this conclusion and indicates that electronic factors affect the geometry of the water coordination. It would appear that while there have been significant advances in the *ab initio* calculations of hexaaqua cations which permit the calculation of trends in a wide range of physical properties there remain problems concerning the calculation of the orientation of the plane of the coordinated water molecule.

An extensive series of large basis set SCF level calculations have recently been published in which ligand-field effects are examined for hydrated divalent and trivalent metal ions of first and second row transition metals [60]. For the trivalent cations the structural and vibrational properties of the caesium sulphate alums provide an excellent test of these calculations since the experimental results have been obtained under equivalent conditions. While the calculations are conducted on *in vacuo* hexaaqua cations, the similarity of the M^{III} site within the alums ought to minimise the usual difficulties which arise when examining trends of this sort. The experimental and calculated M^{III} –O bond lengths are plotted in Fig. 6. The offset between the observed and calculated values (ca. 0.06 \AA) was attributed to the absence of the second coordination sphere about the metal, the hydrogen bonds to which increase the strength of the metal–water bonding [60]. It is important to note that the bond lengths were calculated for hexaaqua cations with T_h symmetry. The significant tilting of the plane of the coordinated water molecule of the Co and Rh hexaaqua cations would appear to have little effect on the bond lengths, consistent with the experimental results discussed above.

The symmetric stretching frequency of the hexaaqua ions has also been calculated and this is shown plotted against the $\nu_1(MO_6)$ vibrational frequency obtained from the caesium sulphate alums in low temperature single-crystal Raman experiments to be described in the following section (Fig. 7). The calculated vibrational frequency was derived by harmonic approximation from the curvature of the potential energy of the system near to the equilibrium bond length. The calculated frequency was

Fig. 6. Calculated vs observed $\text{M}^{\text{III}}-\text{O}$ distances.Fig. 7. Calculated vs observed $\text{M}-\text{OH}_2$ symmetrical stretching frequencies.

found to be sensitive to the choice of fitting points and this is reflected by the error bars. The large offset between the calculated and observed vibrational frequency is due to the absence of consideration of the hydrogen bonding interactions to the second coordination sphere; this both affects the metal–water bond strength and provides a “wall” effect, which raises the observed frequencies above the calculated frequencies.

5. Vibrational spectra

The high symmetry of the alum lattice, the isomorphous replacement of the trivalent metal ions, the substitution of selenate for sulphate and of deuterium for

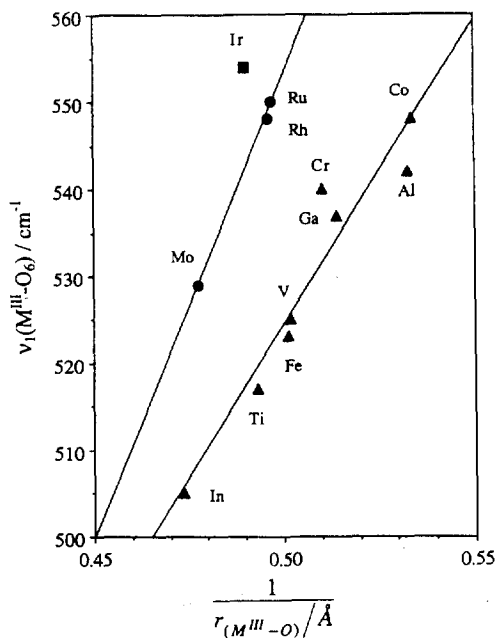


Fig. 8. Correlation of stretching frequency and length of M-O bonds of hexaaquametal(III) ions.

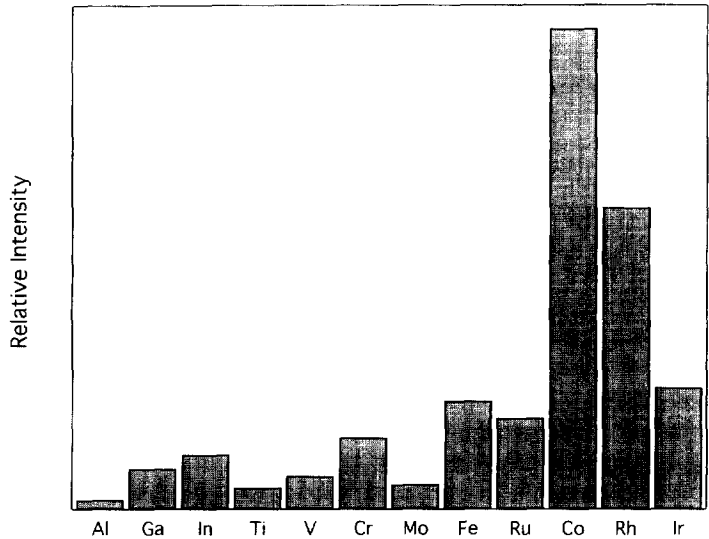


Fig. 9. Relative intensities of A_g components of ν_1 mode of hexaaquametal(III) ions.

hydrogen, and the fortuitous appearance of all, or almost all, of the allowed vibrations of certain symmetries has enabled a comprehensive assignment of the single crystal Raman spectra of many alums [10,68–72]. For example, between 8 and 1200 cm^{-1} factor group analysis predicts that 17 E_g modes should occur, and for $\text{CsAl}(\text{SO}_4)_2 \cdot 12\text{H}_2\text{O}$ all 17 E_g bands are observed. Assignments follow by observing which bands are sensitive or insensitive to substitution of the metal ion, or replacement of H_2O by D_2O , or sulphate by selenate. In this way a self-consistent set of assignments of the E_g modes has been made. The A_g and F_g components are then assigned by association with consideration of the same effects.

There are several noteworthy features of these assignments. One is that they include the very low-frequency lattice modes [72]. Clear distinctions are observed between the α and β alums. There is a correlation between the observed frequencies and the $\text{M}^{\text{III}}\text{O}$ bond length, which reflects the strength of the hydrogen bonds involved in the lattice. A complete normal mode analysis of the alum lattice has not been reported, but the data necessary for it appear to be available.

A second important feature is the availability of the symmetric MO_6 stretching frequencies of the hexaaquametal(III) ions, many for the first time. This ν_1 mode is largely uncoupled from other vibrations and is a direct measure of the metal–water force constant. A linear correlation is observed between the observed frequencies and the inverse of the $\text{M}-\text{O}$ bond lengths (Fig. 8). An unexplained feature of the Raman spectra, however, is the dramatic difference in the intensities of the totally symmetric stretching frequency. This is illustrated in Fig. 9. One speculative correlation is that the intensities are related to the reduction potential of the metal ions, but no proper explanation has been advanced.

The infrared spectra of some of the alums have also been reported [73], but these have not been subject to the same comprehensive analysis as the Raman spectra.

6. Solution structures

Recent neutron scattering experiments conducted on electrolyte solutions containing chromium(III) [74] indicate that the strength of the chromium–water interaction is insensitive to the stereochemistry of water coordination. In $\text{Cr}(\text{ClO}_4)_3$ solutions (2.2 mol dm^{-3}) the tilt of the plane of the coordinated water molecule is reported to be $34 \pm 6^\circ$ with a $\text{Cr}-\text{O}$ bond distance of $1.98(2)\text{ \AA}$ [74]. Whereas the uncertainty of the $\text{Cr}-\text{O}$ distance is too large to permit useful comparison, the frequency of the totally symmetric stretching mode of $[\text{Cr}(\text{OH}_2)_6]^{3+}$, $\nu_1(\text{CrO}_6)$, obtained from Raman spectra of a range of crystals and of solutions of chromium(III) salts give values which are very similar [69]. Since the frequency of $\nu_1(\text{MO}_6)$ is simply related to the $\text{M}-\text{O}$ force constant, the similarity of $\nu_1(\text{MO}_6)$ for the range of different tilt angles for water coordinated to chromium(III) also implies an insensitivity of the metal ligand force constant to the stereochemistry of water coordination.

7. Geometry of the water molecule

The metal–water interaction will influence the electron distribution of the coordinated oxygen atom and this in turn may be expected to influence the geometry of the water molecule. Hydrogen bonding will, of course, contribute to the observed structure. In the most simple case the change from trigonal-planar to trigonal-pyramidal water coordination ought to be accompanied by a reduction in the HOH bond angle. In those cases where accurate neutron structure determinations are available the HOH bond angle is plotted against the metal–water bond length (Fig. 10). It is clear that there is a distinction between the HOH bond angles obtained for the α and β alums with the β alums giving the larger HOH bond angles, as might be expected on the basis of the trigonal-planar mode of water coordination. In order to ascribe this effect to the metal–water interaction it is necessary to establish that this is not a consequence of the hydrogen bonding network of the different alum types. When a broader range of structures is considered, which includes divalent and tervalent hexaaqua cations [78], the trigonal-planar water coordination remains associated with larger values of the HOH bond angle. This suggests that the local structure of the water molecule is expressed even within strongly hydrogen bonding environments.

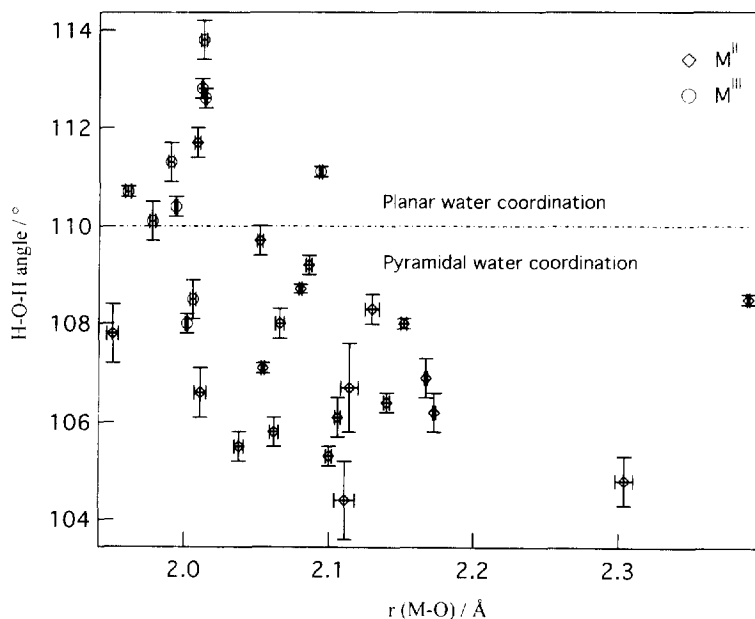


Fig. 10. H-O-H angle dependence of M-O bond length. Data were obtained from $\text{NH}_4\text{Al}(\text{SO}_4)_2 \cdot 12\text{H}_2\text{O}$ [81], the caesium sulphate alums of Cr [14], Fe [13], Mo [82], Ru [17], Rh [78], $\text{Cs}(\text{Fe}(\text{SeO}_4)_2 \cdot 12\text{H}_2\text{O}$ [13], $[\text{V}(\text{OH}_2)_6][\text{H}_5\text{O}_2][\text{CF}_3\text{SO}_3]_4$ [12], $\text{NiSO}_4 \cdot 6\text{H}_2\text{O}$ [83]; and the ammonium Tutton salts of V [84], Cr [85], Mn [86], Fe [87], Ni [88] and Cu [89]. The error bars are drawn at the 1 e.s.d. level.

8. Summary

The interplay between the stereochemistry of the coordinated water molecule and the electronic structure of the tervalent cation has been argued to lie at the heart of the dimorphism of the caesium sulphate alums of titanium(III) and vanadium(III) and has been suggested to influence the geometry of $[\text{V}(\text{OH}_2)_6]^{3+}$ in the salt, $[\text{V}(\text{OH}_2)_6][\text{H}_5\text{O}_2][\text{CF}_3\text{SO}_3]_4$. For the tervalent cations there is an interesting balance between preference for trigonal-planar or trigonal-pyramidal water coordination which is dependent on the metal. This is well illustrated by the alums where three distinct types of behaviour are observed which appear to be linked with the electronic structure of the metal cation. The occupancy of the metal π acceptor orbitals (t_{2g} , O_h) is of key importance. The tervalent cations of Co, Rh and Ir have fully occupied t_{2g} and empty e_g orbitals and only trigonal-pyramidal water coordination has been observed. In cases where there is unequal occupancy of the t_{2g} orbitals trigonal-planar water coordination occurs (Ti, V) and in the remaining cases (Cr, Fe, Al, Ga, In) the mode of water coordination may be either trigonal-planar or trigonal-pyramidal according to the relative energies of the hydrogen bonding arrangements. These observations suggest that in certain cases, at least, the electronic factors arising from the metal–water interaction may influence the stereochemistry of the complex. It is surprising that these preferences may be expressed even in strongly hydrogen bonding environments.

The hexaaqua complexes therefore provide a remarkably beautiful example of the interplay between electronic and molecular structure of metal complexes. In cases where these interactions are in conflict one observes structural anomalies which may be either static (dimorphism of the alums) or dynamic ($\text{CsTi}(\text{SO}_4)_2 \cdot 12\text{H}_2\text{O}$). It is perhaps appropriate that this subtlety be apparent in a venerable series of salts.

Acknowledgments

We acknowledge the considerable contributions of our co-authors in various aspects of this work, especially that of Robert Armstrong of Sydney University in vibrational spectroscopy, Allan White of the University of Western Australia in structure determinations and Philip Tregenna-Piggott for his work on the Ti alum. Some of this work was supported by the Australian Research Grants Scheme.

References

- [1] N.J. Hair, J.K. Beattie, *Inorg. Chem.* 16 (1977) 245.
- [2] B.S. Brunschwig, J. Logan, M.D. Newton, N. Sutin, *J. Am. Chem. Soc.* 102 (1980) 5798.
- [3] F.A. Cotton, L.M. Daniels, C.A. Murillo, J.F. Quesada, *Inorg. Chem.* 32 (1993) 4861.
- [4] D.A. Johnson, A.G. Sharpe, *J. Chem. Soc. Dalton Trans.* (1966) 798.
- [5] S. Haussühl, *Z. Kristallogr.* 116 (1961) 371.
- [6] J.K. Beattie, S.P. Best, B.W. Skelton, A.H. White, *J. Chem. Soc. Dalton Trans.* (1981) 2105.
- [7] H. Lipson, *Proc. R. Soc. A* 151 (1935) 347.

- [8] R.O.W. Fletcher, H. Steeple, *Acta Cryst.* 15 (1962) 960.
- [9] A.H.C. Ledsham, H. Steeple, *Acta Cryst. B* 25 (1969) 398.
- [10] R.S. Armstrong, J.K. Beattie, S.P. Best, B.D. Cole, P.L.W. Tregenna-Piggott, *J. Raman Spectrosc.* 26 (1995) 921.
- [11] G.E. Bacon, W.E. Gardner, *Proc. R. Soc. A* 246 (1958) 78.
- [12] F.A. Cotton, C.K. Fair, G.E. Lewis, G.N. Mott, F.K. Ross, A.J. Schultz, J.M. Williams, *J. Am. Chem. Soc.* 106 (1984) 5319.
- [13] S.P. Best, J.B. Forsyth, *J. Chem. Soc. Dalton Trans.* (1990) 395.
- [14] S.P. Best, J.B. Forsyth, *J. Chem. Soc. Dalton Trans.* (1991) 1721.
- [15] C. Daul, A. Goursot, *Inorg. Chem.* 24 (1985) 3554.
- [16] E. Larsen, G.N. La Mar, *J. Chem. Educ.* 51 (1974) 633.
- [17] S.P. Best, J.B. Forsyth, *J. Chem. Soc. Dalton Trans.* (1990) 3507.
- [18] D. Getz, B.L. Silver, *J. Chem. Phys.* 61 (1974) 630.
- [19] F.A. Wedgwood, *Proc. R. Soc. A* 349 (1976) 447.
- [20] B.N. Figgis, J.B. Forsyth, P.A. Reynolds, *Inorg. Chem.* 26 (1987) 101.
- [21] S.P. Best, B.N. Figgis, J.B. Forsyth, P.A. Reynolds, P.L.W. Tregenna-Piggott, *Inorg. Chem.* 34 (1995) 4605.
- [22] S.W. Lovesey, *Theory of Neutron Scattering from Condensed Matter*, vol. 2, Oxford University Press, Oxford, 1984.
- [23] B.N. Figgis, E.S. Kucharski, G.A. Williams, *J. Chem. Soc. Dalton Trans.* (1980) 1515.
- [24] B.N. Figgis, P.A. Reynolds, *Inorg. Chem.* 24 (1985) 1864.
- [25] P. Schleger, A. Puig-Molina, E. Ressouche, O. Rotty, J. Schweizer, *Acta Cryst. A* to be published.
- [26] R.J. Deeth, B.N. Figgis, J.B. Forsyth, E.S. Kucharski, P.A. Reynolds, *Proc. R. Soc. A* 421 (1989) 153.
- [27] B.N. Figgis, J.B. Forsyth, E.S. Kucharski, P.A. Reynolds, *Proc. R. Soc. A* 428 (1990) 113.
- [28] B.E.F. Fender, B.N. Figgis, J.B. Forsyth, P.A. Reynolds, E. Stevens, *Proc. R. Soc. A* 404 (1986) 127.
- [29] B.E.F. Fender, B.N. Figgis, J.B. Forsyth, *Proc. R. Soc. A* 404 (1986) 139.
- [30] C.D. Delfs, B.N. Figgis, J.B. Forsyth, E.S. Kucharski, P.A. Reynolds, M. Vrtis, *Proc. R. Soc. A* 436 (1992) 417.
- [31] A.B.P. Lever, *Inorganic Electronic Spectroscopy*, Elsevier, Amsterdam, 1968.
- [32] N.S. Hush, R.J.M. Hobbs, *Prog. Inorg. Chem.* 10 (1968) 259.
- [33] C.K. Jørgensen, *Absorption Spectra and Chemical Bonding*, Pergamon Press, Oxford, 1962.
- [34] M.A. Hitchman, R.G. McDonald, P.W. Smith, R. Stranger, *J. Chem. Soc. Dalton Trans.* (1988) 1393.
- [35] S.P. Best, R.J.H. Clark, *Chem. Phys. Lett.* 122 (1985) 401.
- [36] J.K. Beattie, S.P. Best, P. Del Favero, B.W. Skelton, A.N. Sobolev, A.H. White, *J. Chem. Soc. Dalton Trans.* (1996) 1481.
- [37] S. Sugano, I. Tsujikawa, *J. Phys. Soc. Jpn.* 13 (1958) 899.
- [38] R.S. Armstrong, A.J. Berry, B.D. Cole, K.W. Nugent, *J. Chem. Soc. Dalton Trans.* (1997) 363.
- [39] B. Bleaney, *Proc. R. Soc. A* 204 (1950) 203.
- [40] A. Abragam, B. Bleaney, *Electron Paramagnetic Resonance of Transition Metal Ions*, Oxford University Press, Oxford, 1970.
- [41] R.L. Carlin, *Magnetochemistry*, Springer Verlag, Berlin, 1986.
- [42] B.N. Figgis, *Introduction to Ligand Fields*, Wiley, New York, 1966.
- [43] F.E. Mabbs, D.J. Machin, *Magnetism and Transition Metal Complexes*, Chapman and Hall, London, 1973.
- [44] B.N. Figgis, J. Lewis, F.E. Mabbs, *J. Chem. Soc.* (1963) 2473.
- [45] R.J. Benzie, A.H. Cooke, *Proc. R. Soc. A* 209 (1951) 269.
- [46] B. Bleaney, G.S. Bogle, A.H. Cooke, R.J. Duffus, M.C.M. O'Brien, K.W.H. Stevens, *Proc. Phys. Soc. Lond. Ser. A* 68 (1955) 57.
- [47] A. Bose, A.S. Chakravarty, R. Chatterjee, *Ind. J. Phys.* 33 (1959) 325.
- [48] A. Bose, A.S. Chakravarty, R. Chatterjee, *Proc. R. Soc. A* 255 (1960) 145.
- [49] S.K. Dutta-Roy, A.S. Chakravarty, A. Bose, *Ind. J. Phys.* 33 (1959) 483.
- [50] H.M. Gladney, J.D. Swalen, *J. Chem. Phys.* 42 (1965) 1999.
- [51] G.F. Dionne, *Can. J. Phys.* 50 (1972) 2232.
- [52] J.A. Mackinnon, J. Bickerton, *Can. J. Phys.* 48 (1970) 814.

- [53] A. Manoogian, *Can. J. Phys.* 48 (1970) 2577.
- [54] A. Jesion, Y.H. Shing, D. Walsh, in: P.S. Allen, E.R. Andrew, C.A. Bates (Eds.), *Proceedings of the Eighteenth Ampere Congress*, Nottingham, England, 9–14 Sept. 1974, University of Nottingham Press, Nottingham 1975, p. 561.
- [55] Y.H. Shing, W.D. Walsh, *Phys. Rev. Lett.* 33 (1974) 1067.
- [56] H. Tachikawa, A. Murakami, *J. Phys. Chem.* 99 (1995) 11046.
- [57] J. Sygusch, *Acta Cryst. B* 30 (1974) 662.
- [58] P.L.W. Tregenna-Piggott, S.P. Best, M.C.M. O'Brien, K.S. Knight, J.B. Forsyth, J.R. Pilbrow, *J. Am. Chem. Soc.* 119 (1997) to be published.
- [59] L. Dubiki, M.J. Riley, *J. Phys. Chem.* 100 (1997) 1669.
- [60] A. Åkesson, L.G.M. Pettersson, M. Sanström, U. Wahlgren, *J. Am. Chem. Soc.* 116 (1994) 8691.
- [61] G.S. Chandler, G.A. Christos, B.N. Figgis, D.P. Gribble, P.A. Reynolds, *J. Chem. Soc. Faraday Trans. I* (1992) 1953.
- [62] F.P. Rotzinger, *J. Am. Chem. Soc.* 118 (1996) 6760.
- [63] H. Tachikawa, T. Ichikawa, H. Yoshida, *J. Am. Chem. Soc.* 112 (1990) 982.
- [64] A. Åkesson, L.G.M. Pettersson, M. Sanström, U. Wahlgren, *J. Am. Chem. Soc.* 116 (1994) 8705.
- [65] A. Åkesson, L.G.M. Pettersson, M. Sanström, P.E.M. Siegbahn, U. Wahlgren, *J. Phys. Chem.* 97 (1993) 3765.
- [66] P. Brenhard, A. Stebler, A. Ludi, *Inorg. Chem.* 23 (1984) 2151.
- [67] H. Tachikawa, T. Ichikawa, H. Yoshida, *J. Am. Chem. Soc.* 112 (1990) 977.
- [68] S.P. Best, R.S. Armstrong, J.K. Beattie, *J. Chem. Soc. Dalton Trans.* (1982) 1655.
- [69] S.P. Best, J.K. Beattie, R.S. Armstrong, *J. Chem. Soc. Dalton Trans.* (1984) 2611.
- [70] S.P. Best, J.K. Beattie, R.S. Armstrong, G.P. Braithwaite, *J. Chem. Soc. Dalton Trans.* (1989) 1771.
- [71] S.P. Best, R.S. Armstrong, J.K. Beattie, *J. Chem. Soc. Dalton Trans.* (1992) 299.
- [72] J.K. Beattie, R.S. Armstrong, S.P. Best, *Spectrochim. Acta A* 51 (1996) 539.
- [73] S.P. Best, R.S. Armstrong, J.K. Beattie, *Inorg. Chem.* 19 (1980) 1958.
- [74] R.D. Broadbent, G.W. Neilson, S.M. Sanström, *J. Phys., Condens. Matter* 4 (1992) 639.
- [75] A.H.C. Ledsham, H. Steeple, *Acta Cryst. B* 24 (1968) 1287.
- [76] A.C. Larson, D.T. Cromer, *Acta Cryst.* 22 (1967) 793.
- [77] R.S. Armstrong, J.K. Beattie, S.P. Best, B.W. Skelton, A.H. White, *J. Chem. Soc. Dalton Trans.* (1983) 1973.
- [78] J.K. Beattie, S.P. Best, F.H. Moore, B.W. Skelton, A.H. White, *Aust. J. Chem.* 46 (1993) 1337.
- [79] D.T. Cromer, M.I. Kay, A.C. Larson, *Acta Cryst.* 21 (1966) 383.
- [80] D.T. Cromer, M.I. Kay, A.C. Larson, *Acta Cryst.* 22 (1967) 182.
- [81] A.M. Abdeen, G. Will, W. Schäfer, A. Kirfel, M.O. Bargouth, K. Reckre, A. Weiss, *Z. Kristallogr.* 157 (1981) 147.
- [82] S.P. Best, J.B. Forsyth, P.L. Tregenna-Piggott, *J. Chem. Soc. Dalton Trans.* (1993) 2711.
- [83] G.J. McIntyre, H. Ptasiwicz-Bak, I. Olovsson, *Acta Cryst. B* 46 (1990) 27.
- [84] R. Deeth, B.N. Figgis, J.B. Forsyth, E.S. Kucharski, P.A. Reynolds, *Aust. J. Chem.* 41 (1988) 1289.
- [85] B.N. Figgis, J.B. Forsyth, E.S. Kucharski, *Acta Cryst. C* 47 (1991) 419.
- [86] B.E.F. Fender, B.N. Figgis, J.B. Forsyth, P.A. Reynolds, E. Stevens, *Proc. R. Soc. A* 404 (1986) 127.
- [87] B.N. Figgis, E.S. Kucharski, P.A. Reynolds, F. Tasset, *Acta Cryst. C* 45 (1989) 942.
- [88] B.E.F. Fender, B.N. Figgis, J.B. Forsyth, *Aust. J. Chem.* 39 (1986) 1023.
- [89] B.J. Hathaway, A.W. Hewat, *J. Solid State Chem.* 51 (1984) 364.